Surface coils for cardiac imaging using Hyperpolarized ^{13}C at 3 T

W. Dominguez-Viqueira[1], A. Z. Lau[1,2], A. P. Chen[3], and C. H. Cunningham[1,2]
[1]Imaging Research, Sunnybrook Health Sciences Centre, Toronto, Ontario, Canada, [2]Medical Biophysics, University of Toronto, Toronto, Ontario, Canada, [3]GE Healthcare, Toronto, Ontario, Canada

Introduction

Hyperpolarized ^{13}C substrates have become a promising tool to study real-time metabolic processes *in vivo*, particularly in the heart. This was first shown using hyperpolarized ^{13}C pyruvate to characterize cardiac metabolism noninvasively in the pig using a single slice chemical shift imaging (CSI) technique [1]. Recently, rapid multislice imaging of hyperpolarized ^{13}C pyruvate and bicarbonate was demonstrated by Lau et al. [2], using a single shot spiral pulse sequence. To be able to acquire such images rapidly with a good clinical value it is important to optimize the RF coils to obtain the best signal-to-noise ratio (SNR) possible. Even though the sample losses are known to dominate over the coil losses for frequencies higher than 20 MHz, this strongly depends on the coil/sample size [3]. Surface coils offer considerable gains in SNR compared to whole-body coils, but their performance is limited to the volume nearby and up to a distance of about one radius [3]. This is why in the case of surface coils not only the sample and coil losses are important, but also the homogeneity of the RF field through the volume of interest and the distance to it. The objective of this work was to characterize a transmit/receive surface coil for hyperpolarized ^{13}C imaging of in vivo cardiac metabolism in the pig. The quality factors (Q) of the coil loaded and unloaded were measured to estimate the sample/coil losses through the loading factor of the coil. Sensitivity maps of the surface coil were computed and compared to a double channel surface coil design. The actual RF map of the single surface coil was measured by imaging a homogenous spherical phantom and was compared to the theoretical maps. Hyperpolarized ^{13}C pyruvate images of the heart were also obtained to estimate the SNR *in vivo*.

Methods

A custom-built transmit/receive ^{13}C surface coil of 13 cm diameter was used for all the experiments in this work. The quality factors (Q) of the coil in loaded and unloaded conditions were measured using a network analyzer (Agilent Technologies 4395A, USA). The loading measurement was performed by placing the coil over the pig chest in the same position as used for imaging. Three dimensional sensitivity maps of the custom-built coil and a simulated dual-channel surface coil were computed in Matlab (The MathWorks Inc., Massachusetts, USA), by applying Biot-Savart law, and compared.

All imaging experiments were performed on a GE MR750 3T MR scanner (GE Healthcare, Waukesha, WI). Real RF/sensitivity maps of the single transmit/receive surface coil were obtained by imaging a homogenous spherical phantom of 10 cm diameter filled with a mixture of deionized water and ~3 mL of 80 mM hyperpolarized ^{13}C pyruvate. The scan was started 15 s after injection of hyperpolarized ^{13}C to allow mixing, and the SNR maps were compared to the theoretical sensitivity maps computed before. The same sequence (i.e. 48 cm FOV, 8 mm in-plane resolution, 1 cm slice thickness ,single-shot spiral, 16834 samples over 65.5 ms with 250 kHz sampling [2]) was used for imaging hyperpolarized [1-^{13}C] pyruvate in both, phantom and animal studies.

In vivo images were obtained in a specific pathogen free (SPF) pig (25 kg) under a protocol approved by the institutional animal care and use committee. The injection was 15 mL of 83 mM pre-polarized [1-^{13}C] pyruvate as described in [2].

For anatomical landmarking, cardiac-gated breath-held SSFP CINE images were acquired in the short-axis view (TR = 4.2 ms, TE = 1.8 ms, FOV 24 cm, slice thickness 5 mm, spacing 5 mm, matrix size 224×224) using a separate ^{1}H surface coil [2]. *In vivo* hyperpolarized [1-^{13}C] pyruvate images of the heart were acquired using the single-shot cardiac-gated spiral pulse sequence described before. Care was taken not to move the pig when the coil was replaced between proton and ^{13}C acquisitions. The SNR values of ^{13}C images were estimated in multiple region-of-interests (ROIs) using the mean value of the image signal and divided by the standard deviation of the noise in the background.

Results and Discussion

Q factors of 45 and 237 were measured on the single transmit/receive ^{13}C surface coil for loaded and unloaded conditions respectively. This corresponds to a loading factor of 0.81, meaning that in fact the noise is sample dominated and the losses due to the coil are negligible as expected for these frequencies. Figure 1 shows the RF map for the single surface coil (A, B and C) and the two channel surface coil (D, E and F), as simulated in Matlab. The yellow lines represent the RF coils. Due to the planar geometry of the coil the sensitivity decreases with the distance as shown in Fig. 1 (A, B and C), hence the signal drops below the noise floor for the distal regions of the heart. By using a dual coil, with similar dimensions but with positioning along the sides of the pig's chest (Fig. 1 D, E and F) the homogeneity of the RF field can be dramatically improved through the entire heart, permitting a better excitation of the entire volume (e.g. ~same flip angle) and the improvement of the SNR in the posterior part of the heart between 3 and 4 times as seen in Fig. 1 (please note color scale).

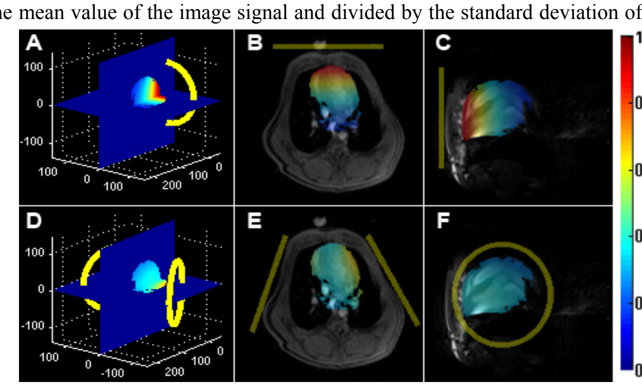

Fig. 1: Magnetic field simulation for the single surface coil (A, B and C) and the two channel surface coil (D, E and F). A and D are the 3D field distribution. B and E are the field distribution overlaid to an axial anatomical image of a pig heart. Similarly C and F are the sagittal field distribution.

Figure 2 shows hyperpolarized [1-^{13}C] pyruvate images and SNR distribution as a function of the distance to the coil for the spherical phantom (A and B) and the pig heart *in vivo* (C and D) using the single transmit/receive surface coil. The experimental results using the homogenous phantom (Fig. 2 A and B) agree well with the simulation results (Fig. 1). The SNR decayed close to zero at a distance of one diameter from the coil as seen in Fig. 2 C and D. A SNR of 44 was measured at the anterior myocardium (i.e. closer to the coil), decaying to 20 by the mid-heart and ~0 by the posterior end as shown in Fig. 2 C and D. Note that the SNR distribution is not only affected by the sensitivity of the coil but also by the effective flip angle throughout the image since the coil is used in transmit/receive mode. However, the SNR measured in the proximal region and the simulation results can be used to predict that a two-coil system would give an SNR of at least 20 throughout the entire heart and possibly higher with a proper flip angle calibration. The best approach would be to use a transmit-only receive-only coil configuration (TORO) using a whole-body transmit coil to ensure the best homogeneity of the RF field and receive the signal using the dual channel coil simulated in this work.

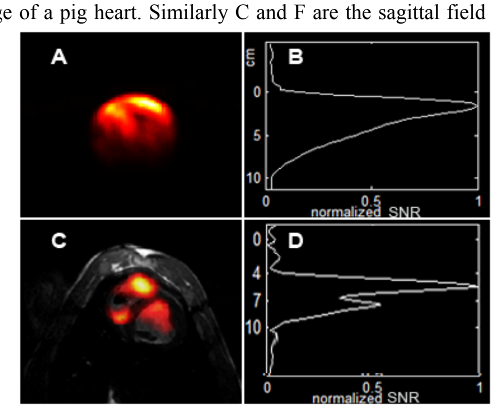

Fig. 2: Real RF distribution measured for the single surface coil in a spherical phantom containing hyperpolarized Pyruvate (A and B) and for an in vivo pyruvate image of a pig heart (C and D).

Conclusions

A single channel ^{13}C transmit/receive surface coil was characterized with benchtop and *in vivo* measurements. Even though sample losses dominate in our experiments, further improvement of the SNR throughout the volume of interest can be achieved by using the dual channel surface coil simulated in this work. This coil configuration will allow the imaging of the different metabolite signals (e.g. [1-^{13}C] pyruvate, [^{13}C] bicarbonate) even in the posterior regions of the myocardium, which is not possible at this moment with the single channel surface coil used in this work. In the near future the dual channel coil simulated in this work will be constructed as well as a full body transmit coil.

References: 1- Golman et al. Magn Reson Med (59) 2008. 2- Lau et al. Magn Reson Med (64) 2010.
3- Doty et al. NMR in biomedicine (20) 2007. 4- Hayes et al. Med. Phys. (12) 1985.